Energetic Materials Frontiers 3 (2022) 146–153

Contents lists available at ScienceDirect

Energetic Materials Frontiers

journal homepage: www.keaipublishing.com/en/journals/energetic-materials-frontiers

Simple and energetic: Novel combination of furoxan and 1,2,4-triazole rings in the synthesis of energetic materials

Alexander A. Larin [a], Ivan V. Ananyev [b,c], Ekaterina V. Dubasova [c,d], Fedor E. Teslenko [a], Konstantin A. Monogarov [e], Dmitry V. Khakimov [a], Chun-lin He [f], Si-ping Pang [f], Galina A. Gazieva [a], Leonid L. Fershtat [a,*]

[a] N.D. Zelinsky Institute of Organic Chemistry, Russian Academy of Sciences, Leninsky Prosp. 47, 119991, Moscow, Russia
[b] N.S. Kurnakov Institute of General and Inorganic Chemistry, Russian Academy of Sciences, GSP-1, Leninsky Prosp. 31, 119991, Moscow, Russia
[c] A.N. Nesmeyanov Institute of Organoelement Compounds, Russian Academy of Sciences, Vavilova Str. 28, 119991, Moscow, Russia
[d] D.I. Mendeleev University of Chemical Technology of Russia, Miusskaya Sq. 9, 125047, Moscow, Russia
[e] N.N. Semenov Federal Research Center for Chemical Physics, Russian Academy of Sciences, Kosygin Str. 4, 119991, Moscow, Russia
[f] School of Materials Science & Engineering, Beijing Institute of Technology, Beijing, 100081, China

ARTICLE INFO

Keywords:
Nitrogen heterocycles
Energetic materials
1,2,5-Oxadiazoles
Mechanical sensitivity
Electrostatic potential

ABSTRACT

Two novel representatives of energetic (1,2,4-triazolyl)furoxans were prepared from the readily available (furoxanyl)amidrazones. Synthesized compounds were thoroughly characterized with IR and multinuclear NMR spectroscopy, elemental analysis and X-ray diffraction data. Analysis of structural features supported by quantum-chemical calculations revealed the main reasons for experimentally observed difference in thermal stability and mechanical sensitivity of both compounds. It was found that 3-cyano-4-(1*H*-1,2,4-triazol-3-yl)furoxan is more thermally stable (T_d: 229 °C) than 4-azido-3-(1*H*-1,2,4-triazol-3-yl)furoxan (T_d: 154 °C) and the latter compound is also more sensitive to impact and friction. In addition, both heterocyclic assemblies have high detonation parameters (v_D: 7.0–8.0 km·s^{-1}; *p*: 22–29 GPa) exceeding those of benchmark explosives trinitrotoluene and hexanitrostilbene which enable their usability for various energetic applications.

1. Introduction

Energetic materials constitute one of the most important class of functional materials used for various applications, such as mining, explosion welding, preparation of propellants and fuels.[1,2] To meet the growing demand for different applications, large numbers of energetic materials have been developed.[3–10] However, advanced space and civilian technologies bring new increased requirements to the synthesis and performance of High Energy Density Materials (HEDMs).[11,12] Novel energetic materials should have balanced functional properties including good detonation performance, high density and high enthalpy of formation. At the same time, such materials should possess moderate sensitivity toward various mechanical stimuli to guarantee safety concerns associated with their preparation, isolation and handling. Therefore, a search of novel high-energy materials with balanced criteria is constantly required.

In a recent decade, promising results in the development of energetic materials were achieved upon assembly of polynitrogen and nitrogen-oxygen biheterocyclic structures.[13–19] Such materials usually have high enthalpies of formation and more balanced functional properties. In a series of such polyheteroatom heterocyclic compounds, a combination of the furazan (1,2,5-oxadiazole) or furoxan (1,2,5-oxadiazole 2-oxide) and 1,2,4-triazole motifs may become a promising platform for the preparation of novel energetic materials.[20] Several preliminary results demonstrated that this biheterocyclic (1,2,4-triazolyl)-1,2,5-oxadiazole framework contributes to the optimal balance between high detonation performance and acceptable mechanical sensitivity of the resulted energetic materials.[21,22] Herein, we report on the synthesis, structural characterization, physicochemical and detonation properties of novel (1,2,4-triazolyl)furoxans bearing cyano and azido functionalities at the furoxan ring (Fig. 1).

2. Experimental section

CAUTION! Although we have encountered no difficulties during preparation and handling of the compounds described in this paper, they

* Corresponding author.
E-mail address: fershtat@bk.ru (L.L. Fershtat).

https://doi.org/10.1016/j.enmf.2022.08.002
Received 24 April 2022; Received in revised form 4 June 2022; Accepted 9 August 2022
Available online 17 August 2022

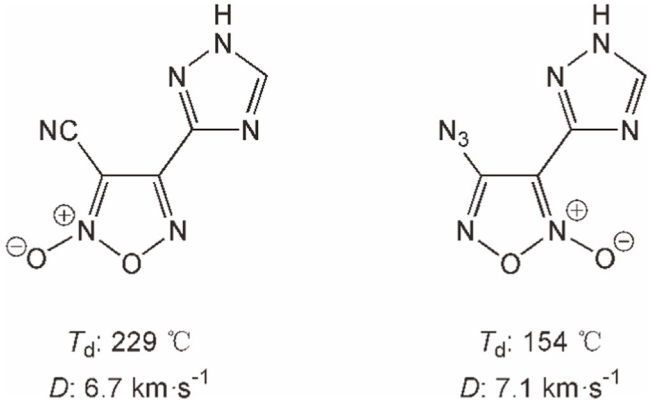

Fig. 1. Previously known and newly synthesized energetic (1,2,4-triazolyl)-1,2,5-oxadiazoles.

are potentially explosive energetic materials that are sensitive to impact and friction. Mechanical actions of these energetic materials, involving scratching or scraping, must be avoided. Any manipulations must be carried out by using appropriate standard safety precautions.

2.1. General methods

All reactions were carried out in well-cleaned oven-dried glassware with magnetic stirring. ^{1}H and ^{13}C NMR spectra were recorded with a Bruker AM-300 (300.13 MHz and 75.47 MHz, respectively) spectrometer and referenced to the residual solvent peak. ^{15}N NMR spectra were recorded with a Bruker DRX500 instrument (the frequency for ^{15}N was 50.7 MHz) at room temperature. The chemical shifts are reported in ppm (δ). The IR spectra were recorded with a Bruker "Alpha" spectrometer in the range 400–4000 cm^{-1} (resolution 2 cm^{-1}). Elemental analyses were performed by the CHN Analyzer PerkinElmer 2400. All solvents were purified and dried by standard methods prior to use. All standard reagents were purchased from Aldrich or Acros Organics and used without further purification. **2a**[23] and **2b**[24] were synthesized according to the literature.

2.2. Thermal analysis and sensitivity measurements

Thermal analysis of the substances was carried out with a Netzsch STA 449 F3 apparatus. Samples (0.2–3 mg, depending on their heat release rate) were poured in alumina pans covered with pierced lids. Investigated samples were heated up to 600 °C with a constant rate of 5 K·min^{-1}. Impact sensitivity tests were performed by using a BAM-type machine according to STANAG 4489. The reported values (IS) are the drop energies corresponding to 50% probability of explosion obtained with Bruceton analysis. Friction sensitivity was evaluated in agreement with STANAG 4487. Reported quantity (FS) is the friction force corresponding to 50% probability of explosion obtained with Bruceton analysis.

2.3. X-ray diffraction data

X-ray diffraction data for crystals of **3a**·H_2O and **3b** were measured using the Bruker APEX II diffractometer equipped with the Photon 2 detector (MoKλ-radiation, graphite monochromator, ω-scans). The intensity data were integrated by the SAINT program[25] and were corrected for absorption and decay using SADABS.[26] Both structures were solved by direct methods using SHELXS[27] and refined using the full matrix least squares technique against F^2 using SHELXL-2018.[28] Positions of hydrogen atoms were found from the difference Fourier synthesis of electron density. Non-hydrogen and hydrogen atoms were refined in the anisotropic and isotropic approximations, respectively. The main refinement details and parameters are given in the Table S2 in ESI. CCDC 2167747–2167748 contain all additional supplementary data.

2.4. Computational details

The enthalpy of formation calculations were carried out combining the atomization energy method[29,30] (eq. (1)) with CBS-QB3 electronic enthalpies.[31,32] CBS-QB3 energies of the atoms were calculated with the Gaussian09 software package.[33] Values for $\Delta_f H^\circ$ (atoms) were taken from the NIST database.

$$\Delta_f H^\circ_{(g,\ 298)} = H^o_{(Molecule,\ 298)} - \sum H^\circ_{(Atoms,\ 298)} + \sum \Delta_f H^\circ_{(Atoms,\ 298)} \quad \text{(eq 1)}$$

Where $\Delta_f H^\circ_{(g,\ 298)}$ is the calculated enthalpy of formation in the gas phase, H^o (molecule) is the calculated enthalpy of a molecule formation, H^o (atoms) – the enthalpy of the calculated values of atoms, ΔH_f^o (atoms) – the experimental enthalpy of formation for the atoms in the gas phase.

Geometric optimization of all structures for crystal packing calculation was carried out using the DFT/B3LYP functional and the aug-cc-PVDZ basis set with a Grimme's D2 dispersion correction.[34] The optimized structures were conformed to be true local energy minima on the potential-energy surface by frequency analyses at the same level.

In the calculation of lattice energy, the molecules were treated as rigid bodies with foxed point groups. We applied pairwise atom-atom potentials to describe the van der Waals and electrostatic point charges for Coulomb components of intermolecular energy. At the initial stage '6–12' Lennard-Jones (LJ) type potential parameters were used.[35] The electrostatic energy was calculated with a set of displaced point charge sites by program FitMEP.[36] The lattice energy simulations were performed with the program PMC.[37]

Enthalpies of sublimation for **3a** and **3b** were calculated by formula:

$$\Delta H_{subl} = -E_{lat} - 2RT \quad \text{(eq 2)}$$

where R is the universal gas constant, E_{lat} is the lattice energy, T is temperature (298 K).

The DFT calculations of isolated molecules of **3a** and **3b** were performed using the Gaussian 09 program (rev. D01)[33] at the PBE0[38,39]/-def2TZVP level with the Grimme's D3 dispersion corrections and Becke-Jonson damping.[40] Standard convergence criteria were used for the optimization procedures. The crystal conformation of **3b** was calculated with the optimization of only hydrogen atom positions. The equilibrium and flat isolated structures of **3b** were calculated by the full optimization starting from, respectively, crystal structure and flattened structure with furoxan and triazolyl cycles lying in the same plane. For all isolated systems, the type of saddle point on potential energy surface were confirmed by the calculations of Hessian of electronic energy (ultrafine grids, no imaginary modes were found with the only exception of the flat structure). The Interacting Quantum Atoms calculations were done using the AIMAll program.[41]

The computations of intermolecular energy frameworks and lattice energies (clusters of more than 50 independent units were used) as well as the calculations and analysis of Hirshfeld surfaces were done within the CrystalExplorer program.[42] The density of **3a** molecule in **3a**·$\mathbf{H_2O}$ was estimated using the QTAIM atomic volumes calculated for the cluster isolated from **3a**·$\mathbf{H_2O}$ crystal structure. The cluster was generated by surrounding of the **3a** molecule by all molecular units forming contacts with lengths smaller than sum of vdW radii and 5 Å. The electron density function for the cluster was calculated at the HF/3-21G level (lengths of X–H bonds were normalized). The integration procedure was done using the MultiWFN program.[43]

2.5. General procedure for the preparation of *3a* and *3b*

p-Toluenesulfonic acid monohydrate (112 mg, 0.59 mmol) was added at room temperature to the stirred solution of **2a,2b** (5.9 mmol) and trimethyl orthoformate (3 mL, 29.5 mmol) in dry CH_3CN (13 mL). After

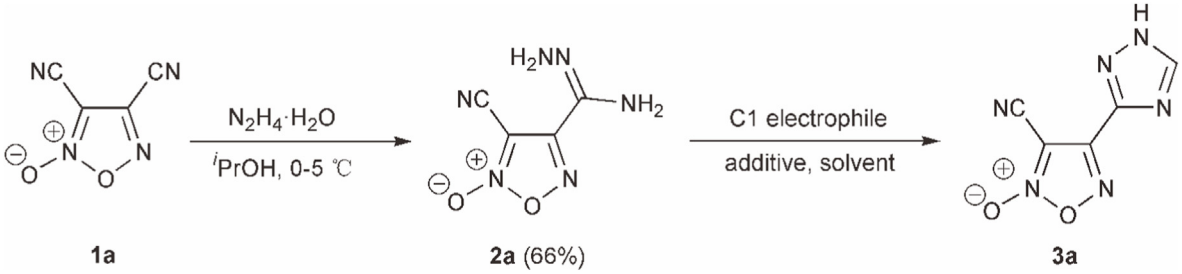

Scheme 1. Synthesis of energetic 3-cyano-4-(1,2,4-triazol-3-yl)furoxan (**3a**).

Table 1
Optimization of the reaction conditions for the synthesis of **3a**.

Entry	Reagent (equiv.)	Additive (equiv.)	Solvent	*T*/°C	Time/h	Yield[a]/%
1	$Me_2N–CH(OMe)_2$ (1)	–	Dioxane	102	24	-[b]
2	EtOCH = NH·HCl (1)	$BF_3·Et_2O$ (10 mol %)	MeOH	60	6	-[b]
3	EtOCH = NH·HCl (1.1)	Na_2CO_3 (1.1)	H_2O	50	10	-[b]
4	EtOCH = NH·HCl (1.1)	–	AcOH	120	6	-[b]
5	$HC(OMe)_3$ (5)	$ZnCl_2$ (10 mol %)	MeOH	40	20	-[b]
6	$HC(OMe)_3$ (5)	$ZnCl_2$ (10 mol %)	MeCN	40	20	-[b]
7	$HC(OMe)_3$ (5)	–	MeOH	20	20	25
8	$HC(OMe)_3$ (5)	$BF_3·Et_2O$ (10 mol %)	MeCN	40	15	48
9	$HC(OMe)_3$ (8)	$BF_3·Et_2O$ (10 mol %)	MeCN	40	20	45
10	$HC(OMe)_3$ (8)	$BF_3·Et_2O$ (20 mol %)	MeCN	40	25	44
11	$HC(OMe)_3$ (8)	$Sc(OTf)_3$ (10 mol %)	MeCN	20	2	56
12	$HC(OMe)_3$ (5)	$Sc(OTf)_3$ (10 mol %)	MeCN	40	1.5	80
13	$HC(OMe)_3$ (5)	PTSA•H_2O (10 mol %)	MeCN	40	1.5	95
14	$HC(OMe)_3$ (6)	PTSA•H_2O (10 mol %)	MeCN	50	1.5	92

[a] Isolated yields are given.
[b] No reaction.

10 min, the reaction mixture was heated to 40 °C and stirred for additional 1.5 h (TLC monitoring, eluent $CHCl_3$–EtOAc, 1:1). Dark red solution obtained in the case of **3a** was cooled and poured into ice water (50 mL), extracted with EtOAc (3 × 80 mL), combined organic extracts were washed with brine (2 × 50 mL) and dried over $MgSO_4$. In the case of **3b** the reaction mixture was evaporated to dryness, the residue was washed with cold water (2 × 10 mL) and cold EtOAc (2 × 10 mL) and dried in air.

3-Cyano-4-(1*H*-1,2,4-triazol-3-yl)furoxan (**3a**): Yield 0.99 g (95%); light orange solid; R_f 0.31 ($CHCl_3$-EtOAc, 1:1); ^{1}H NMR (300 MHz, [D_6]DMSO) δ: 14.98 (br s, 1H), 8.97 (s, 1H); ^{13}C NMR (75.5 MHz, [D_6]DMSO) δ: 149.7, 149.0, 146.5, 107.1, 98.1; ^{15}N NMR (60.8 MHz, [D_6]DMSO) δ: −11.1, −18.3, −86.9, −94.4, −131.6, −159.4; IR (KBr, ν/cm^{-1}): 3144, 3085, 2856, 2253, 1632, 1610, 1521, 1454, 1278, 1178, 1106, 1057; elemental analysis calcd (%) for $C_5H_2N_6O_2$ (178.03): C 33.72, H 1.13, N 47.19; found: C 33.49, H 1.29, N 46.87; IS: 19 J, FS: 220 N.

4-Azido-3-(1*H*-1,2,4-triazol-3-yl)furoxan (**3b**): Yield 0.92 g (81%); white solid; R_f 0.46 ($CHCl_3$-EtOAc, 1:1); ^{1}H NMR (300 MHz, [D_6]DMSO) δ: 14.86 (s, 1H), 8.86 (s, 1H); ^{13}C NMR (75.5 MHz, [D_6]DMSO) δ: 153.0, 147.2, 146.1, 105.5[14]; N NMR (21.7 MHz, [D_6]DMSO) δ: −146.5 (br. s, N_3); IR (KBr, ν/cm^{-1}): 3137, 2858, 2164, 1633, 1545, 1519, 1415, 1268, 1200, 1022; elemental analysis calcd (%) for $C_4H_2N_8O_2$ (194.04): C 24.75, H 1.04, N 57.73; found: C 24.93, H 0.88, N 57.49; IS: 4.2 J, FS: 270 N.

3. Results and discussion

3.1. Synthesis

For the synthesis of desired (1,2,4-triazolyl)furoxans, dicyanofuroxan (**1a**) and 4-azido-3-cyanofuroxan (**1b**) were chosen as readily available

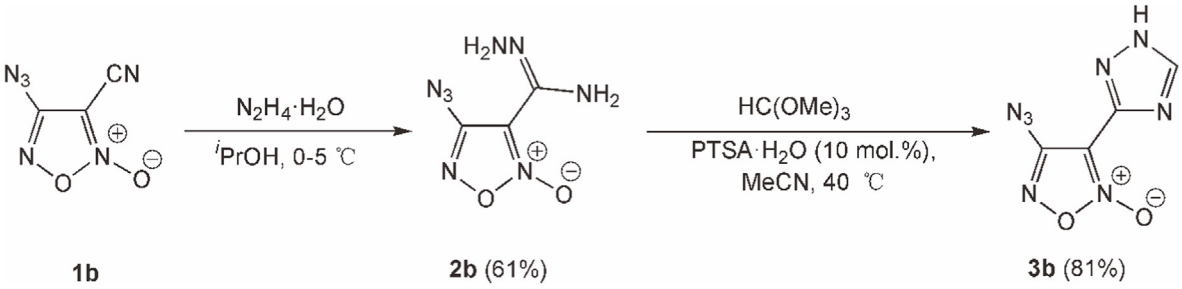

Scheme 2. Synthesis of energetic 4-azido-3-(1,2,4-triazol-3-yl)furoxan (**3b**).

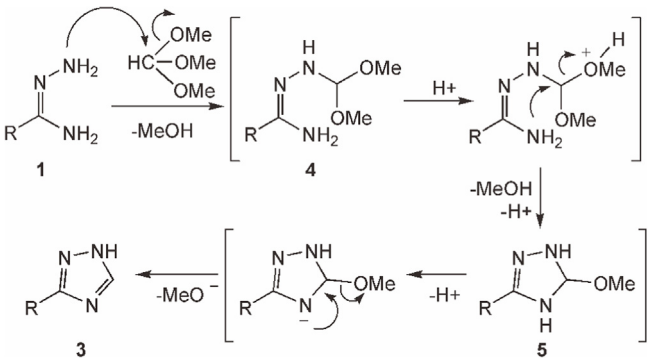

Scheme 3. A plausible mechanism for an assembly of the 1,2,4-triazole ring.

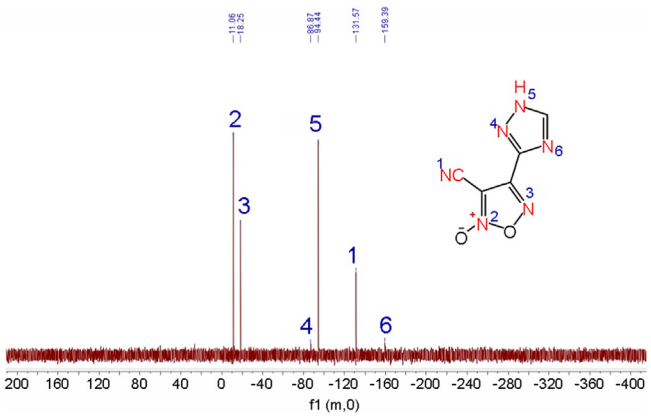

Fig. 2. ^{15}N NMR spectrum of compound **3a**.

starting materials. **1a** was converted to the corresponding **2a** *via* an interaction with hydrazine-hydrate according to the known procedure (Scheme 1).[23] Then an optimization of the reaction conditions for an assembly of the 1,2,4-triazole ring was performed (Table 1). Our attempts to construct 1,2,4-triazole ring using dimethylformamide dimethylacetal or ethyl formimidate hydrochloride in a combination with various additives in different solvents were unsuccessful (entries 1–4). Utilization of trimethyl orthoformate in the presence of $ZnCl_2$ was also useless (entries 5,6). Interestingly, performing the reaction with an excess of trimethyl orthoformate in MeOH without any additives afforded target product **3a** in a low yield. Further screening of various acidic catalysts (entries 7–14) demonstrated that the highest yield of the product **3a** was achieved upon using 10 mol.% *p*-toluenesulfonic acid monohydrate (PTSA•H_2O) in MeCN at 40 °C (entry 13).

Under optimized conditions, **2b** synthesized from the corresponding **1b** was subjected to the studied cyclization. Target **3b** was prepared in a good yield (Scheme 2).

A plausible mechanism for an assembly of the 1,2,4-triazole ring is outlined in Scheme 3. Initial condensation of **1** with trimethyl orthoformate results in a generation of **4** which after protonation undergoes ring formation. Then, **5** eliminates MeOH molecule to furnish the formation of target **3**.

3.2. Structure determination

The structures of the synthesized **3a** and **3b** were confirmed by IR and multinuclear NMR spectroscopy, elemental analysis and X-ray diffraction studies. 3-Cyano-4-(1,2,4-triazolyl)furoxan (**3a**) was additionally characterized by ^{15}N NMR spectroscopy (Fig. 2). The chemical shift of *N*-oxide nitrogen atom is located more downfield (−11.1) in comparison with another furoxan ring nitrogen atom (−18.3). The signal of the nitrile group occurred at −131.6 and the presence of all three nitrogen atoms of the 1,2,4-triazole ring is also in agreement with the previously reported values.[21]

As only the hydrate form of **3a** has been successfully crystallized (**3a**·H_2O), the quantum chemical calculations have been also invoked to shed some light on the relation between peculiarities of crystal structures and detonation properties. According to X-ray diffraction data, the conformations of (1,2,4-triazolyl)furoxans are pronouncedly different in crystals of **3a**·H_2O and **3b** (Fig. 3). The **3a** molecule is nearly planar with the mean and maximal deviations from the mean-squared plane composed by non-hydrogen atoms equal to 0.035 Å and 0.099 Å, respectively (the rotation of triazolyl plane against the furoxan cycle is less than 5°). This conformation is evidently stabilized by π-conjugation effects which also play the key role in the isolated state: the r.m.s. Difference between experimental geometry and the structure optimized in the isolated state at the PBE0-D3/def2tzvp level is only 0.052 Å (for non-hydrogen atoms, see Fig. S1 in ESI). In contrast, the crystal conformation of **3b** is characterized by a pronounced rotation of triazolyl (28.3(2)°) and azide (10.6(2)°) fragments with respect to furoxan plane in **3b**. Moreover, the **3b** molecule is bent along the C1–C3 bond: the C1 and C3 atoms go out of the planes of triazolyl and furoxan cycles on 0.126(3) and 0.131(3) Å, respectively. The PBE0-D3/def2tzvp calculations show that the crystal conformation of **3b** can be formally rationalized by the combination of steric repulsion effects and the influence of intermolecular forces. Indeed, the triazolyl fragment is also rotated against the furoxan cycle in the isolated **3b** molecule, although to a lesser extent (16.3°, Fig. S1 in ESI). At the same time, even the accounting for non-specific solvation (scrf-pcm model, $\varepsilon = 72$) was not able to reproduce the other features of crystal conformation of **3b**, i.e. the bending along the C1–C3 bond and the rotation of azide moiety.

According to the inspection of intermolecular energy frameworks[44] calculated at the CE-B3LYP/6-31G(d,p) level, the crystal packing of **3b** is of anisotropic character (Fig. 4). The main contributions to the total crystal lattice energy (up to 110.5 kJ·mol^{-1} from total 133.9 kJ·mol^{-1}) raise from the interactions within layers of molecules. According to Zhang et al.,[45] the anisotropic type of crystal packing is believed to decrease the sensitivity of HEDM towards impact that contradicts with the rather low value of impact sensitivity measured for **3b** (see below Table 2). This contradiction can be, however, resolved by the thorough analysis of supramolecular organization and its influence on the conformational preferences of **3b**.

The analysis of crystal packing of **3b** based on the geometry criteria has revealed two types of shortened intermolecular contacts corresponding to H-bonds and π … π stacking interactions (Fig. 5). The triazolyl fragments participate in rather strong N–H···N H-bonds (N4···N5 2.842(3) Å, ∠(NHN) 159.9°) which aggregate molecules into infinite chains. The layers composed by those chains are stabilized by weak azide … triazolyl C–H···N hydrogen bonds (C4···N6 3.684(3) Å, ∠(CHN) 166.9°) and stacking interactions between furoxan and triazole moieties. Note, that the stacking interactions are characterized both by rather short interatomic contacts (C1···N3 3.184(3) Å, C4···N3 3.138(3) Å) and not perfect (face-to-face) configuration with a small area of overlap between heterocycles. The geometry of supramolecular aggregation of H-bonded chains supports both conformational features observed for **3b** in crystal: the bending and the rotation along the C1–C3 bond can be the result of stacking interactions, while the rotation of azide moiety is favored by the C4–H···N6 H-bond. In its turn, this conformation of **3b** results in the non-parallel arrangement of molecules within the layers that a) may increase the rigidity of crystal packing against mechanical deformations and b) leads to an isotropic distribution of types of intermolecular contacts. Indeed, the distribution of d_{norm} values mapped on the Hirshfeld surface[46] of **3b** molecule is rather flat (with the exception of N–H···N H-bonds, Fig. 6) while the distribution of type of contacts crossing the Hirshfeld surface is characterized by a negative kurtosis (−1.64, see Fig. S2 and Table S1 in ESI).

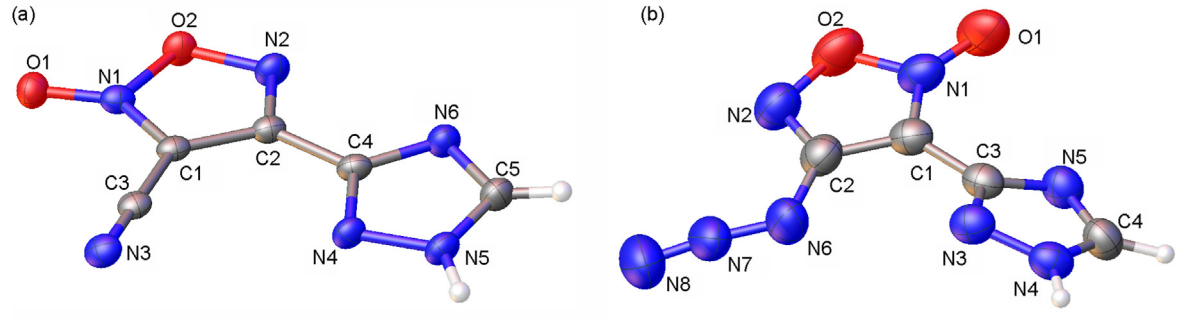

Fig. 3. Molecular structures of **3a** (a) and **3b** (b) in crystals of **3a**·H_2O and **3b**, respectively. Non-hydrogen atoms are drawn as atomic displacement ellipsoids at the $p = 0.5$ level.

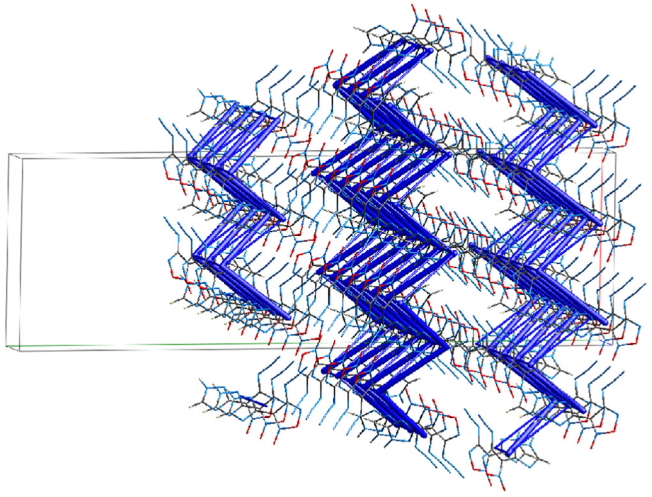

Fig. 4. The intermolecular energy frameworks for **3b** crystal calculated at the CE-B3LYP/6-31G(d,p) level (tube size 45, cut-off value 15.5 kJ·mol^{-1}).

One can assume that the distorted conformation of azido(1,2,4-triazolyl)furoxan in crystal does not only favors more gripped packing with isotropic molecular environment but may play its own role in the high impact sensitivity of this HEDM. The energy difference between crystal (only H atoms were optimized) and isolated equilibrium conformations equals to 11.3 kJ•mol^{-1}. This considerable deformation energy is in line with the rather large value of crystal lattice energy (see above) and is primarily the consequence of intermolecular perturbations. Indeed, the energy difference between the isolated equilibrium **3b** molecule and the flat structure with furoxan and triazole cycles lying in the same plane (saddle point of first order on potential energy surface) is less than 0.4 kJ•mol^{-1} that prevents from considering the steric effects as the meaningful factor influencing the **3b** conformation. Noteworthy, the decomposition of energy within the Interatomic Quantum Atoms approach[47] suggests that the interatomic interactions play the leading role in stabilization of non-favorable conformation of **3b** in crystal: while the intraatomic self energies increase upon the transition from flat structure to equilibrium and further to the crystal conformation (on 8.8 kJ•mol^{-1} and 92.9 kJ•mol^{-1}, respectively), it is the energy of interactions between atoms that attempts to stabilize the system (on 8.8 kJ•mol^{-1} and 82.0 kJ•mol^{-1}, correspondingly).

Unfortunately, the available data on crystal structure of **3a** in its hydrate form (**3a**·H_2O) cannot be directly compared with the **3b** structure to elucidate the difference in impact sensitivity of two studied (triazolyl)furoxans. However, some preliminary suppositions on the influence of crystal structural features of **3a** on its detonation related properties can still be made based on the quantum chemical calculations and the Hirshfeld surface analysis. For instance, the density of **3a** molecule in its crystal was estimated using the known Δ_{OED}-technique[48–50] which is based on the QTAIM partition[51] of the crystal structure. The obtained value (1.67 g•cm^{-3}) is somewhat larger than the density of **3a**·H_2O (1.623 g·cm^{-3} according to X-ray diffraction data measured at 100 K) and agrees satisfactory with the density of water-free sample of **3a** measured by gas pycnometer at room temperature (1.55 g•cm^{-3}). The rather small density values for **3a** can be considered as the manifestation of its tendency to form strong H-bonds which are known to prevent molecules for close aggregation.[52] Indeed, the inspection of **3a**·H_2O crystal has revealed that the infinite chains stabilized by strong H-bonds between triazolyl fragment and water molecules are

Table 2
Physical properties and detonation parameters.

Compound	T_d[a]/°C	ρ[b]/g cm^{-3}	Ω_{CO}[c]/%	N + O[d]/%	$\Delta H^0_{f,solid}$[e]/kJ mol^{-1}	IS[f]/J	FS[g]/N	v_D[h]/km•s^{-1}	p[i]/GPa
3a	229	1.55	−36.0	65.2	453	19	220	7.0	22
3b	154	1.70	−24.7	74.2	623	4	270	8.0	29
TNT	275[54]	1.64	−24.7	60.8	−62[55]	30[54]	>360[54]	6.9	23
HNS	318[48]	1.75	−17.8	61.3	78[48]	5[48]	360[48]	7.6	24

[a] Decomposition temperature (DSC, 5 K·min^{-1}).
[b] Density measured by gas pycnometer (298 K).
[c] Oxygen balance (based on CO) for $C_aH_bO_cN_d$, 1600(c-a-b/2)/MW.
[d] Nitrogen-oxygen content.
[e] Calculated enthalpy of formation.
[f] Experimental impact sensitivity obtained in present study.
[g] Experimental friction sensitivity obtained in present study.
[h] Detonation velocity.
[i] Detonation pressure.

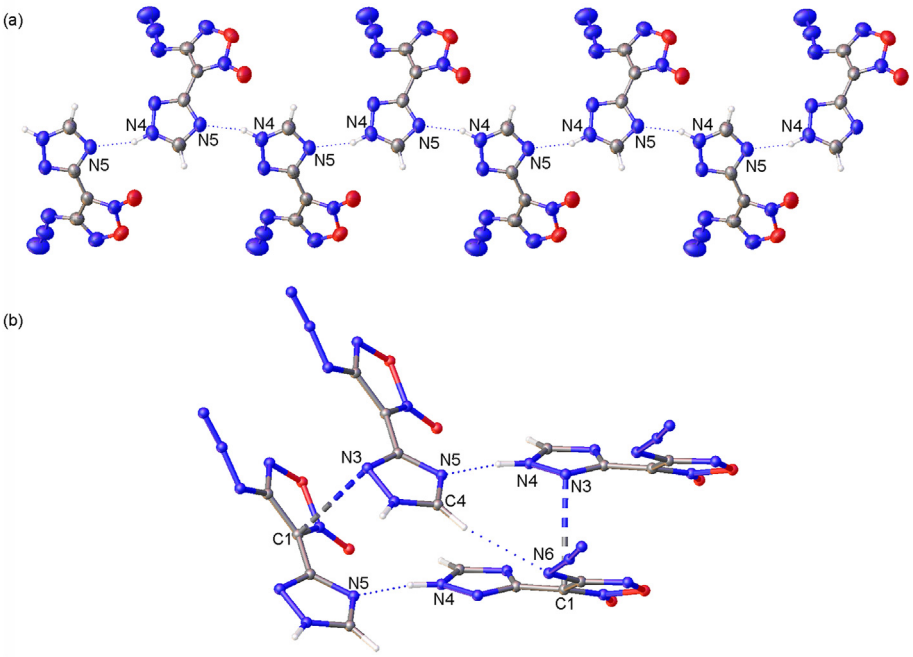

Fig. 5. The fragment of infinite H-bonded chain (a) and the main intermolecular interactions within layers (b) in the crystal of **3b**. H-bonds and stacking interactions are depicted by dotted and dashed lines, respectively.

the main motif of crystal packing (Fig. 7): N5···O1W 2.670(2) Å, ∠(NHO) 169.9°, N6···O1W 2.809(2) Å, ∠(NHO) 178.9°. The chains are hold together by weak H-bond with the nitrile moiety (N3···O1W 3.038(2) Å, ∠(NHO) 157.3°) and multiple O … π interactions. Despite the absence of pronounced layer motif and stacking interaction in **3a**·H_2O (in comparison with **3b**), the pie-like shape of Hirshfeld surface of **3a** in this crystal (Fig. 6) together with the distribution of corresponding d_{norm} values (the kurtosis of distribution of contacts crossing the surface is positive, Fig. S2 and Table S1 in ESI) agree well with the low impact sensitivity of the water-free sample (see below).

3.3. Physicochemical and energetic properties

The physical and detonation properties, such as thermal stability, density, enthalpy of formation, detonation performance, as well as sensitivity of all target compounds, were investigated. The results are summarized in Table 2. Thermal stability of compound **3a** bearing cyano functionality is rather high, *viz.*, the extrapolated onset is 229 °C. The introduction of azido group predictably lowers the decomposition onset, to 154 °C. Both compounds have high combined nitrogen-oxygen contents (65–74%) and positive enthalpies of formation (453–623 kJ·mol^{-1}). Friction sensitivity of both materials is not much different, and its magnitude is less than that of common nitramine explosives. Impact sensitivity values are in accordance with thermal safety data: **3a** is less sensitive than **3b**. Detonation performance was computed with empirical methods included in PILEM application (PILEM is Predictive Laboratory of Energetic Materials).[53] **3a** showed good detonation performance (v_D: 7.0 km•s^{-1}; *p*: 22 GPa) comparable to trinitrotoluene (v_D: 6.9 km•s^{-1}; *p*: 23 GPa), while **3b** demonstrated even higher detonation properties (v_D: 8.0 km•s^{-1}; *p*: 29 GPa) exceeding those of benchmark hexanitrostilbene.

The calculated electrostatic potentials (ESP) of both **3a** and **3b** are shown in Fig. 8. Maximum positive values of ESP are quite similar for both compounds **3a** and **3b** (223.2 kJ•mol^{-1} and 237.1 kJ•mol^{-1}, respectively) and are located at NH fragment of the 1,2,4-triazole ring which are attributed to the acidic properties of 1,2,4-triazoles bearing electron-withdrawing substituents (e.g. furoxan ring). On the contrary, maximum negative values of ESP differ more significantly and are located between the N(4) nitrogen atom of the 1,2,4-triazole ring and the furoxan motif (−119.5 kJ•mol^{-1} for **3a** and −175.4 kJ•mol^{-1} for **3b**). Such difference raised from much weaker delocalization of the negative charge in **3b** which is connected to the closer disposition of the *N*-oxide functionality and the 1,2,4-triazole motif and results in higher impact sensitivity[56] (4 J) of this compound compared to that of **3a** (19 J). In addition, the high sensitivity of **3b** could be explained by the depletion of

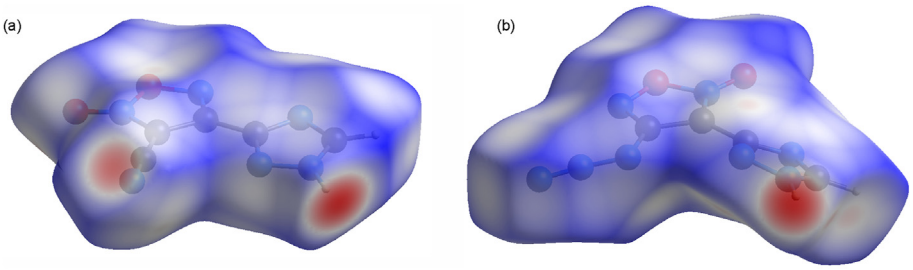

Fig. 6. The Hirshfeld surfaces colored by the d_{norm} values for the **3a** and **3b** molecules in **3a**·H_2O and **3b** crystals, respectively.

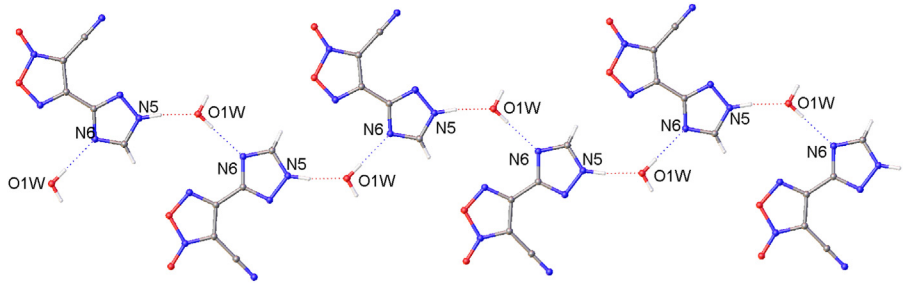

Fig. 7. The fragment of infinite H-bonded chain in crystal of **3a**.

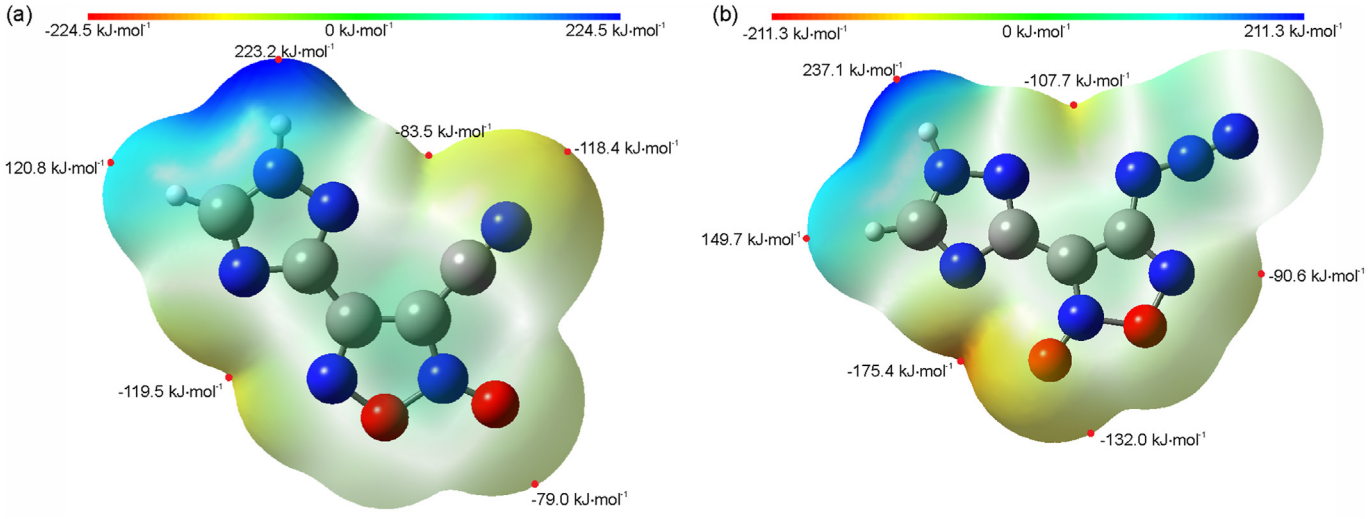

Fig. 8. Molecular electrostatic potentials of compounds **3a** (a) and **3b** (b) calculated with B3LYP/6-31G(*d*,*p*) basis set.

electronic charge caused by the sensitive azido group, which would cause the increase of electropositive area in compound **3b**.

4. Conclusions

In conclusion, novel energetic compounds comprised of the furoxan and 1,2,4-triazole rings enriched with cyano or azido functionalities were synthesized. Both compounds were fully characterized using IR and multinuclear NMR spectroscopy, elemental analysis and X-ray diffraction study. Unfavored supramolecular organization and higher negative electrostatic potential of 4-azido-3-(1,2,4-triazolyl)furoxan (**3b**) are responsible for lower thermal stability and higher impact sensitivity of this compound in comparison with the cyano derivative **3a**. Nevertheless, **3a** showed good detonation performance (v_D: 7.0 km·s^{-1}; *p*: 22 GPa) comparable to trinitrotoluene (v_D: 6.9 km·s^{-1}; *p*: 23 GPa), while 4-azido-3-(1*H*-1,2,4-triazol-3-yl)furoxan (**3b**) demonstrated even higher detonation properties (v_D: 8.0 km·s^{-1}; *p*: 29 GPa) exceeding those of benchmark hexanitrostilbene.

Declaration of competing interest

The authors declare that they have no known competing financial interests or personal relationships that could have appeared to influence the work reported in this paper.

Acknowledgements

A.A. Larin, K.A. Monogarov and G.A. Gazieva are grateful to the Russian Science Foundation (grant 19-73-20074) for the financial support of synthetic studies, estimation of thermal stability and sensitivity measurements of energetic materials reported in this work. I.V. Ananyev and E.V. Dubasova are grateful to the Russian Science Foundation (project 22-13-00238) for the financial support of X-ray diffraction studies, quantum chemical calculations, interacting quantum atoms and QTAIM computations and the analysis of Hirshfeld surfaces.

Appendix A. Supplementary data

Supplementary data to this article can be found online at https://doi.org/10.1016/j.enmf.2022.08.002.

References

1. O'Sullivan OT, Zdilla MJ. Properties and promise of catenated nitrogen systems as high-energy-density materials. *Chem Rev*. 2020;120(12):5682–5744.
2. Ma X, Li Y, Hussain I, Shen R, Yang G, Zhang K. Core–shell structured nanoenergetic materials: preparation and fundamental properties. *Adv Mater*. 2020;32(30), 2001291.
3. Das J, Shem-Tov D, Zhang S, et al. Power of sulfur – chemistry, properties, laser ignition and theoretical studies of energetic perchlorate-free 1,3,4-thiadiazole nitramines. *Chem Eng J*. 2022;443, 136246.
4. Sabatini JJ, Johnson EC. A short review of nitric esters and their role in energetic materials. *ACS Omega*. 2021;6(18):11813–11821.
5. Das J, Shem-Tov D, Wang S, et al. Hydride- and boron-free solid hypergolic H_2O_2-ignitophores. *Chem Eng J*. 2021;426, 131806.
6. Luo S-N, Gozin M. Energetic materials: novel syntheses and diagnostics. *Engineering*. 2020;6(9):974–975.
7. Larin AA, Fershtat LL. High-energy hydroxytetrazoles: design, synthesis and performance. *Energ Mater Front*. 2021;2(1):3–13.
8. Tarchoun AF, Trache D, Klapötke TM, Khimeche K. Tetrazole-functionalized microcrystalline cellulose: a promising biopolymer for advanced energetic materials. *Chem Eng J*. 2020;400, 125960.

9. Snyder CJ, Imler GH, Chavez DE, Parrish DA. Synergetic explosive performance through cocrystallization. *Cryst Growth Des*. 2021;21(3):1401–1405.
10. Zlotin SG, Churakov AM, Egorov MP, et al. Advanced energetic materials: novel strategies and versatile applications. *Mendeleev Commun*. 2021;31(6):731–749.
11. Klapötke TM. *Energetic Materials Encyclopedia*. Berlin: De Gruyter; 2018.
12. Klapötke TM. *Chemistry of High-Energy Materials*. third ed. Berlin: De Gruyter; 2015.
13. Larin AA, Shaferov AV, Monogarov KA, Meerov DB, Pivkina AN, Fershtat LL. Novel energetic oxadiazole assemblies. *Mendeleev Commun*. 2022;32(1):111–113.
14. Larin AA, Bystrov DM, Fershtat LL, et al. Nitro-, cyano-, and methylfuroxans, and their bis-derivatives: from green primary to melt-cast explosives. *Molecules*. 2020; 25(24):5836.
15. Larin AA, Shaferov AV, Epishina MA, et al. Pushing the energy-sensitivity balance with high-performance bifuroxans. *ACS Appl Energy Mater*. 2020;3(8):7764–7771.
16. Muravyev NV, Melnikov IN, Chaplygin DA, Fershtat LL, Monogarov KA. Two sides of thermal stability of energetic liquid: vaporization and decomposition of 3-methylfuroxan. *J Mol Liq*. 2022;348, 118059.
17. Fershtat LL, Ovchinnikov IV, Epishina MA, et al. Assembly of nitrofurazan and nitrofuroxan frameworks for high-performance energetic materials. *ChemPlusChem*. 2017;82(11):1315–1319.
18. Voronin AA, Fedyanin IV, Churakov AM, et al. 4*H*-[1,2,3]Triazolo[4,5-*c*][1,2,5] oxadiazole 5-oxide and its salts: promising multipurpose energetic materials. *ACS Appl Energy Mater*. 2020;3(9):9401–9407.
19. Yount JR, Zeller M, Byrd EFC, Piercey DG. 4,4'',5,5''-Tetraamino-3,3''-azo-bis-1,2,4-triazole and the electrosynthesis of high-performing insensitive energetic materials. *J Mater Chem*. 2020;8(37):19337–19347.
20. Fershtat LL, Makhova NN. 1,2,5-Oxadiazole-based high-energy-density materials: synthesis and performance. *ChemPlusChem*. 2020;85(1):13–42.
21. Xu Z, Cheng G, Yang H, et al. A facile and versatile synthesis of energetic furazan-functionalized 5-nitroimino-1,2,4-triazoles. *Angew Chem Int Ed*. 2017;56(21): 5877–5881.
22. Li Y, Zhang Z, Ge Z, Wang B, Lai W, Luo Y. Study of furoxan derivatives for energetic applications. *Chin J Chem*. 2013;31(4):520–524.
23. Fershtat LL, Epishina MA, Ovchinnikov IV, Kachala VV, Makhova NN. An effective synthesis of (1*H*-1,2,4-triazol-3-yl)furoxans. *Chem Heterocycl Compd*. 2015;51(8): 754–759.
24. Larin AA, Shaferov AV, Kulikov AS, et al. Design and synthesis of nitrogen-rich azo-bridged furoxanylazoles as high-performance energetic materials. *Chem Eur J*. 2021; 27(59):14628–14637.
25. *Bruker. APEX-III*. Madison, Wisconsin, USA: Bruker AXS Inc.; 2018.
26. Krause L, Herbst-Irmer R, Sheldrick GM, Stalke DJ. Comparison of silver and molybdenum microfocus X-ray sources for single-crystal structure determination. *J Appl Crystallogr*. 2015;48(1):3–13.
27. Sheldrick GM. SHELXT-integrated space-group and crystal-structure determination. *Acta Crystallogr A*. 2015;71(1):3–8.
28. Sheldrick GM. Crystal structure refinement with SHELXL. *Acta Crystallogr C*. 2015; 71(1):3–8.
29. Montgomery JJA, Frisch MJ, Ochterski JW, Petersson GA. A complete basis set model chemistry. VII. Use of the minimum population localization method. *J Chem Phys*. 2000;112(15):6532–6542.
30. Ochterski JW, Petersson GA, Montgomery JJA. A complete basis set model chemistry. V. Extensions to six or more heavy atoms. *J Chem Phys*. 1996;104(7): 2598–2619.
31. Klapötke TM. Computational methods. In: *Chemistry of High-Energy Materials*. Berlin–Boston: Walter de Gruyter; 2012:89.
32. Khakimov DV, Dalinger IL, Pivina TS. *J Comput Theor Chem*. 2015;1063(1):24–28.
33. Frisch MJ, Trucks GW, Schlegel HB, et al. *Gaussian 09, Revision D.01*. Wallingford CT: Gaussian, Inc.; 2016.
34. Grimme S. Density functional theory with London dispersion corrections. *WIREs Comput Mol Sci*. 2011;1(2):211–228.
35. Momany FA, Carruthers LM, McGuire RF, Scheraga HA. Intermolecular potentials from crystal data. III. Determination of empirical potentials and application to the packing configurations and lattice energies in crystals of hydrocarbons, carboxylic acids, amines, and amides. *J Phys Chem*. 1974;78(16):1595–1620.
36. Dzyabchenko AV. A multipole approximation of the electrostatic potential of molecules. *Russ J Phys Chem A*. 2008;82(5):758.
37. Dzyabchenko AV. From molecule to solid: the prediction of organic crystal structures. *Russ J Phys Chem A*. 2008;82(10):1663–1671.
38. Perdew J, Ernzerhof M, Burke K. Rationale for mixing exact exchange with density functional approximations. *J Chem Phys*. 1996;105(22):9982–9985.
39. Carlo A, Barone V. Toward reliable density functional methods without adjustable parameters: the PBE0 model. *J Chem Phys*. 1999;110(13):6158–6170.
40. Grimme S, Ehrlich S, Goerigk L. Effect of the damping function in dispersion corrected density functional theory. *J Comput Chem*. 2011;32(7):1456–1465.
41. AIMAll (Version 19.10.12) Todd A, Keith TK. *Gristmill Software*. Overland Park KS, USA. 2019 (aim.tkgristmill.com).
42. Spackman PR, Turner MJ, McKinnon JJ, et al. CrystalExplorer: a program for Hirshfeld surface analysis, visualization and quantitative analysis of molecular crystals. *J Appl Crystallogr*. 2021;54(3):1006–1011.
43. Lu T, Chen F. Multiwfn: a multifunctional wavefunction analyzer. *J Comput Chem*. 2012;33(5):580–592.
44. Mackenzie CF, Spackman PR, Jayatilaka D, Spackman MA. CrystalExplorer model energies and energy frameworks: extension to metal coordination compounds, organic salts, solvates and open-shell systems. *IUCrJ*. 2017;4(5):575–587.
45. Tian B, Xiong Y, Chen L, Zhang C. Relationship between the crystal packing and impact sensitivity of energetic materials. *CrystEngComm*. 2018;20(6):837–848.
46. Spackman MA, Jayatilaka D. Hirshfeld surface analysis. *CrystEngComm*. 2009;11(1): 19–32.
47. Blanco MA, Pendás AM, Francisco E. Interacting quantum atoms: a correlated energy decomposition scheme based on the quantum theory of atoms in molecules. *J Chem Theor Comput*. 2005;1(6):1096–1109.
48. Larin AA, Muravyev NV, Pivkina AN, et al. Assembly of tetrazolylfuroxan organic salts: multipurpose green energetic materials with high enthalpies of formation and excellent detonation performance. *Chem Eur J*. 2019;25(16):4225–4233.
49. KYu Suponitsky, Smol'yakov AF, Ananyev IV, Khakhalev AV, Gidaspov AA, Sheremetev AB. 3,4-Dinitrofurazan: structural nonequivalence of ortho-nitro groups as a key feature of the crystal structure and density. *ChemistrySelect*. 2020;5(46): 14543–14548.
50. KYu Suponitsky, Fedyanin IV, Karnoukhova VA, et al. Energetic co-crystal of a primary metal-free explosive with BTF. Ideal pair for co-crystallization. *Molecules*. 2021;26(24):7452.
51. Matta CF, Boyd RJ. *The Quantum Theory of Atoms in Molecules: From Solid State to DNA*. Drug Design. Weinheim: Wiley-VCH Verlag GmbH & Co. KgaA; 2007.
52. Gidaspov AA, Zalomlenkov VA, Bakharev VV, et al. Novel trinitroethanol derivatives: high energetic 2-(2,2,2-trinitroethoxy)-1,3,5-triazines. *RSC Adv*. 2016;6(41): 34921–34934.
53. Muravyev NV, Wozniak D, Piercey DG. Progress and performance of energetic materials: open dataset, tool, and implications for synthesis. *J Mater Chem*. 2022; 10(20):11054–11073.
54. Muravyev NV, Meerov DB, Monogarov KA, et al. Sensitivity of energetic materials: evidence of thermodynamic factor on a large array of CHNOFCl compounds. *Chem Eng J*. 2021;421(1), 129804.
55. Muravyev NV, Monogarov KA, Melnikov IN, Pivkina AN, Kiselev VG. Learning to fly: thermochemistry of energetic materials by modified thermogravimetric analysis and highly accurate quantum chemical calculations. *Phys Chem Chem Phys*. 2021;23(29): 15522–15542.
56. Kang Y, Dong Y, Liu Y, Gao H, Wang Y, Shreeve JM. Halogen bonding (C-F···X) and its effect on creating ideal insensitive energetic materials. *Chem Eng J*. 2022;440, 135969.

Alexander A. Larin graduated from the Lomonosov Moscow State University in 2015 (Department of Chemistry). He received his Ph.D. degree from the N. D. Zelinsky Institute of Organic Chemistry in 2019 under the supervision of Prof. N. N. Makhova. Currently, he is a researcher in the same institute. His scientific interests include development of novel synthetic methodologies in the field of nitrogen-containing heterocycles, especially, high-energy 1,2,5-oxadiazoles 2-oxides (furoxans). E-mail: roby3@mail.ru

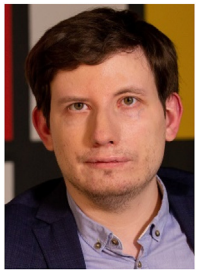

Leonid L. Fershtat graduated from the D.I. Mendeleev University of Chemical Technology in 2012 (faculty Higher Chemical College of the Russian Academy of Sciences). He received his Ph.D. degree from the N. D. Zelinsky Institute of Organic Chemistry in 2015 under the supervision of Prof. N. N. Makhova. In 2020, he finished his habilitation studies in the same institute. Dr. Fershtat is serving as an Associate Editor of the *Energetic Materials Frontiers* journal (Elsevier), a Member of the Editorial Boards of the *Defense Technology* and *FirePhysChem* journals (Elsevier), and a Member of an Early Career Advisory Board in *Mendeleev Communications* (Elsevier). His scientific interests include a creation of novel methodologies in the synthesis and transformations of nitrogen-containing heterocycles, and search for pharmacologically active and high energy heterocyclic derivatives. Orcid.org/0000-0002-0203-1025; E-mail: fershtat@bk.ru